ADVANCING EARTH AND SPACE SCIENCES

JGR Atmospheres

RESEARCH ARTICLE
10.1029/2023JD039006

Key Points:

- Oxygen stable isotope ($\delta^{18}O$) records from the new Huascarán ice cores strongly reflect Pacific climate variability of the most recent 60-year
- Tropical Pacific influences on the Huascarán $\delta^{18}O$ records have strengthened significantly in the last six decades
- $\delta^{18}O$ from the higher elevation Summit appears to be more sensitive to large-scale climate change than $\delta^{18}O$ from the lower-elevation Col

Supporting Information:

Supporting Information may be found in the online version of this article.

Correspondence to:

A. M. Weber,
weber.1158@osu.edu

Citation:

Weber, A. M., Thompson, L. G., Davis, M., Mosley-Thompson, E., Beaudon, E., Kenny, D., et al. (2023). Drivers of $\delta^{18}O$ variability preserved in ice cores from Earth's highest tropical mountain. *Journal of Geophysical Research: Atmospheres*, *128*, e2023JD039006. https://doi.org/10.1029/2023JD039006

Received 3 APR 2023
Accepted 15 SEP 2023

Author Contributions:

Conceptualization: A. M. Weber, L. G. Thompson
Data curation: L. G. Thompson, M. Davis
Formal analysis: A. M. Weber
Funding acquisition: L. G. Thompson, E. Mosley-Thompson
Investigation: A. M. Weber, E. Beaudon, D. Kenny, P.-N. Lin, R. Sierra-Hernández
Methodology: A. M. Weber
Project Administration: L. G. Thompson, E. Mosley-Thompson
Resources: L. G. Thompson, M. Davis

Drivers of $\delta^{18}O$ Variability Preserved in Ice Cores From Earth's Highest Tropical Mountain

A. M. Weber[1,2], L. G. Thompson[1,2], M. Davis[1], E. Mosley-Thompson[1,3], E. Beaudon[1], D. Kenny[1], P.-N. Lin[1], and R. Sierra-Hernández[1]

[1]Byrd Polar and Climate Research Center, Columbus, OH, USA, [2]School of Earth Sciences, The Ohio State University, Columbus, OH, USA, [3]Department of Geography, The Ohio State University, Columbus, OH, USA

Abstract In 2019, four ice cores were recovered from the world's highest tropical mountain, Nevado Huascarán (Cordillera Blanca, Peru; 9.11°S, 77.61°W). Composite hydroclimate records of the two Col cores (6,050 masl) and the two Summit cores (6,768 masl) are compared to gridded gauge-analysis and reanalysis climate data for the most recent 60-year. Spatiotemporal correlation analyses suggest that the ice core oxygen stable isotope ($\delta^{18}O$) record largely reflects tropical Pacific climate variability, particularly in the NINO3.4 region. By extension, the $\delta^{18}O$ record is strongly related to rainfall over the Amazon Basin, as teleconnections between the El Niño Southern Oscillation and hydrological behavior are the main drivers of the fractionation of water isotopes. However, on a local scale, modulation of the stable water isotopes appears to be more closely governed by upper atmospheric temperatures than by rainfall amount. Over the last 60 years, the statistical significance of the climate/$\delta^{18}O$ relationship has been increasing contemporaneously with the atmospheric and oceanic warming rates and shifts in the Walker circulation. Isotopic records from the Summit appear to be more sensitive to large-scale temperature changes than the records from the Col. These results may have substantial implications for modeling studies of the behavior of water isotopes at high elevations in the tropical Andes.

Plain Language Summary The oxygen stable isotope records ($\delta^{18}O$) of the new Huascarán ice cores (collected in 2019 from Peru) are a natural archive of tropical Pacific climate and hydrological conditions over the Amazon Basin. This is evidenced by strong correlations between $\delta^{18}O$ and spatiotemporal sea surface temperature (SST) and precipitation data sets that cover the most recent 60 years of the ice core records. Additionally, the Huascarán $\delta^{18}O$ records are significantly related to temperatures in the upper atmosphere, suggesting that temperature may also play a critical role in modifying the isotope values. The statistical significance of each of these relationships has also been increasing over the last 60 years, and the rates of increase are greatest between the $\delta^{18}O$ records from the higher elevation ice core site and the temperature-related climate data sets. This suggests that the isotope records from the Huascarán Summit (6,768 masl) are more sensitive to large-scale changes in temperature than the isotope records on the Huascarán Col (6,050 masl). This is the first study to examine ice core records from the Summit of Earth's highest tropical mountain and offers valuable insights into the behavior of $\delta^{18}O$ in the tropical Andes.

1. Introduction

Tropical regions play a critical role in Earth's climate system (Cai et al., 2019), and better understandings of past changes in tropical climates can improve predictions of future climate patterns and impacts. The proxy records preserved in ice cores provide valuable tools for reconstructing paleoclimates as they can provide insights into prehistoric temperatures, precipitation, and atmospheric circulation. In particular, the oxygen stable isotope ($\delta^{18}O$) records from tropical ice cores can be very useful for estimating such parameters. For instance, Vuille et al. (2003) used observational records and a pair of general circulation models to show that the $\delta^{18}O$ records from tropical Andean ice cores function as a proxy of tropical Pacific climate. These findings are supported by the work of Thompson et al. (2013), who identified a strong correlation between $\delta^{18}O$ in the Quelccaya ice cores (13.93°S, 70.83°W, and 5,670 masl) and 140 years of sea surface temperature (SST) data for the NINO4 region of the equatorial Pacific. From their analysis of the Quelccaya isotopes the authors established a connection between Pacific climate and the migration of the intertropical convergence zone (ITCZ) and also reconstructed a 1.8 ka history of NINO4 SSTs. Additional ice core $\delta^{18}O$ records from the tropical Andes have been linked to upper atmosphere zonal winds (Henderson et al., 1999) and temperatures (Thompson et al., 2017), as well as hydrological conditions over the Amazon Basin (Ampuero et al., 2020; Ramirez et al., 2003; da Rocha Ribeiro et al., 2018).

10.1029/2023JD039006

Software: A. M. Weber
Supervision: L. G. Thompson
Validation: A. M. Weber, M. Davis
Visualization: A. M. Weber
Writing – original draft: A. M. Weber
Writing – review & editing: A. M. Weber, L. G. Thompson, M. Davis, E. Mosley-Thompson, E. Beaudon, D. Kenny, P.-N. Lin, R. Sierra-Hernández

These different climatic conditions are interrelated via ocean-air interactions and/or the Walker circulation over South America (Barichivich et al., 2018; Veiga et al., 2005).

The goal of this study is to expand the discussion of the tropical climate parameters recorded in low latitude, high altitude ice cores by introducing two new composite records collected in 2019 from the Col (6,050 masl) and Summit (6,768 masl) of Nevado Huascarán, Earth's highest tropical mountain. While previous studies examined two ice cores recovered from the Huascarán Col in 1993 (Thompson et al., 1995), no ice cores were obtained from the mountain Summit until the 2019 field expedition. As such, this study introduces the first-ever analysis of oxygen isotope records from the Huascarán Summit and provides an invaluable perspective on the behavior of water isotopes within different atmospheric layers on the same tropical mountain. Moreover, the data presented here provide a 26-year update to the records of the original Huascarán ice cores drilled in 1993. This extension allows for more robust analyses of our interpretations of how modern climate is archived by glacial ice at this location. The re-drilling of Huascarán also validates the reproducibility of the isotopic measurements of the 1993 cores, which are very highly correlated with the new Col cores (see Text S1 in Supporting Information S1). Furthermore, the new highly resolved temporal and spatial $\delta^{18}O$ observations presented here could greatly improve isotopic modeling, which is particularly challenging because of the dramatic topography of the Andes.

Here, we present the most recent six decades (1960–2019) of annually resolved $\delta^{18}O$ records from the new HS ice cores and evaluate their spatiotemporal relationships with respect to modern SST, precipitation, and upper atmosphere temperature data. Our findings offer significant insights into the understanding of how $\delta^{18}O$ is preserved in glacial ice at multiple elevations on HS and how it relates to modern understandings of isotope fractionation processes in tropical South America. Section 2 describes the methodology for collecting the ice cores and summarizes both the dating of the cores and the procedures for employing gridded climate data sets in our analysis. Section 3 presents the general results of our SST, precipitation, and upper atmosphere temperature analyses. Section 4 discusses the multidecadal trends in the $\delta^{18}O$/climate relationships. Section 5 briefly covers the linkages between $\delta^{18}O$ and various oceanic oscillations. Finally, Section 6 summarizes the main results and provides our key takeaways.

2. Materials and Methods

2.1. Study Region

Nevado Huascarán (HS) is located in the Cordillera Blanca (CB) mountain range of the Peruvian Andes (Figure 1). Due to its high elevation topography and local meteorological conditions, the CB contains the largest concentration of glacial ice in the global tropics (USGS, 1999). However, HS is unlike other high elevation sites in the area as the $\delta^{18}O$ records preserved in the surface snow are currently unaltered by local warming rates (Thompson et al., 2017, 2021). This makes HS an ideal site for ice core research and was thus a motivator for the original ice retrieval mission conducted in 1993 (Thompson et al., 1995) and the most recent drilling campaign in 2019 during which two cores were drilled from both the Col and the Summit drill sites.

Although the CB is geographically much closer to the Pacific Ocean, most of the moisture transported to the Peruvian Andes originates in the tropical North Atlantic (Eghdami & Barros, 2019; Grootes et al., 1989). During the CB wet season (October through April), a pressure cell known as the Azores High directs northeasterly winds carrying water vapor across the South American continent (Figure 1). The southward migration of the ITCZ is linked to warmer SSTs in the South Atlantic Ocean (Córdova et al., 2022) and further channels moist air to the Chaco Low, which is associated with an upper level anticyclone (the Bolivian High; Figueroa et al., 1995; Junquas et al., 2018) that diverts moist air westward to the Andes (Valdivielso et al., 2020). Roughly 90% of the total annual precipitation in the CB is generated during the wet season (Vuille et al., 2008), leaving May through September considerably drier. In contrast to this wet/dry seasonality, the mean air temperature in the CB is very stable. For instance, according to Llanganuco station (3,835 masl) records in the valley north of HS, mean air temperatures hover around 8.0°C ± 2.5°C throughout the year (Mateo et al., 2022).

Delivery of atmospheric moisture across tropical South America is aided by evaporative recycling over the Amazon Basin. The Amazon Basin contains an estimated 5.3 million km^2 of moist tropical forests (Marengo et al., 2018), the dense canopies of which are integral to the regional hydrological cycle and the westward advection of water vapor. Continental forests are essential for the maintenance of atmospheric moisture over land as evidenced by an exponential decrease in precipitation with distance from the ocean in non-forested environments

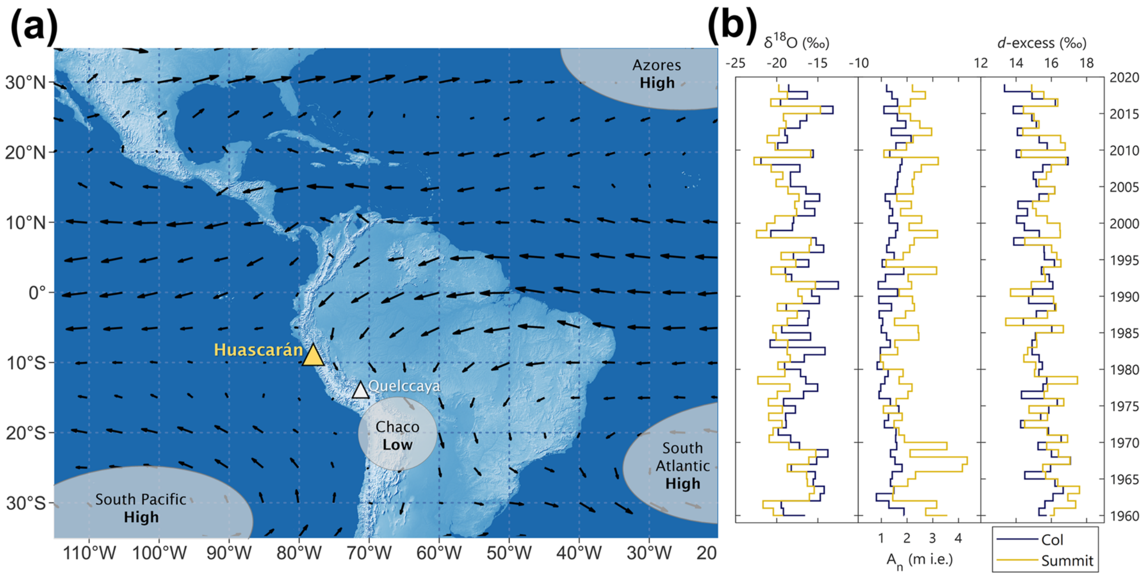

Figure 1. (a) Schematic diagram of atmospheric conditions during the CB wet season. Black arrows depict the average 750 hPa winds during DJF 2015–2019 (ERA5, https://cds.climate.copernicus.eu/#!/home). (b) The annual HS ice core records are on the right, given as composites of the two Col and two Summit cores.

(Makarieva et al., 2009). According to an early modeling study by Eltahir and Bras (1994), as much as 35% of the rainfall across the Amazon is recycled through evapotranspiration. Recent estimates, based on Lagrangian simulations using data from ERA5, reveal a similar precipitation recycling rate of 36% for the Amazon Basin (Tuinenburg et al., 2020).

2.2. The Ice Cores

The 2019 expedition to HS successfully recovered four ice cores to bedrock. Two of the cores were extracted from the HS Col (6,050 masl)—the same site that was drilled 26 years earlier—while the remaining two cores were retrieved from the HS Summit (6,768 masl). The Summit ice cores are the highest elevation cores ever collected from the tropics.

All four cores were returned frozen to the Byrd Polar and Climate Research Center (BPCRC) at the Ohio State University where they are stored in a −34°C freezer. To establish an accurate timeline for interpreting the records, each core was subsampled vertically using the procedure described by Weber (2022). The full length of each core and the number of individual samples is given in Table S1 in Supporting Information S1. All samples were melted and analyzed for $\delta^{18}O$ and stable isotopes of hydrogen (δD) at the BPCRC using a Picarro L2140-i cavity ringdown spectrometer. Deuterium excess (*d*-excess) was calculated by the equation [$d\text{-excess} = \delta D - 8 \times \delta^{18}O$]. Additional samples, co-registered with depth, were cut simultaneously with the $\delta^{18}O$ samples and were washed and melted in a Class 100 Clean Room at the BPCRC for analysis of ion and microparticle concentrations. Ions were measured chromatographically with a Dionex ICS 5000 while the microparticle concentrations and size distributions were determined with a Beckman Coulter Multisizer 4. Both instruments are also housed in the Class 100 Clean Room.

The highly resolved seasonal peaks in $\delta^{18}O$, nitrate, and microparticles (dust) were used to construct an annual time series for the uppermost layers of each core. The dating process for Col Core B is thoroughly described in Section 2.2 and Figures 3 and 4 of Weber (2022), and the same procedure was utilized for the remaining three cores. The individual $\delta^{18}O$, nitrate, and dust concentration measurements are of sufficiently high enough resolution to distinguish the wet and dry seasonal cycles at HS, thus the annual layer dating between 1960 and 2019 has an accuracy of virtually ±0 thermal years. For the HS ice cores a thermal year timeline is used, which assumes that the peak of the dry season occurs in July of the previous year. For instance, the 2000 thermal year is defined as the period from July 1999 to July 2000. The use of a thermal year calendar as opposed to the standard Gregorian calendar should have a negligible effect on our analyses, as explained in Section 2.2.

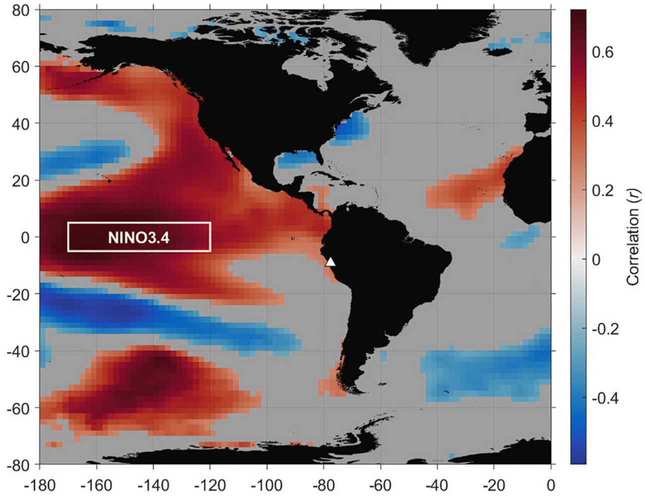

Figure 2. Spatial correlation field (2° × 2°) between HS $\delta^{18}O_{col}$ and the October through April ERSSTs for the period 1960–2019. Only the grid cells that are statistically significant at the 95% level (p-value ≤0.05) are plotted. The white triangle denotes the location of the ice core site.

Once the timescales for the ice core records were constructed, the values of each of the parameters ($\delta^{18}O$, nitrate, dust) were averaged by year to create an annual data set for each core. Composite records for the two Col cores and the two Summit cores were produced by taking the mean value for each year. For example, the average $\delta^{18}O$ values for the 2015 thermal year in Col Core A and Col Core B were −16.32‰ and −16.39‰, respectively. The mean of these two values (−16.36‰) was thus used as the final value for the 2015 thermal year in the Col composite record. The composite records are considered more representative of the "true" annual values than the individual records, thus the composite records for the Col and Summit are what we use in the analyses that follow.

Details of our reconstruction of net annual accumulation rates (A_n) in the HS ice cores are given in Text S2 in Supporting Information S1. Here, we focus on the annually averaged HS record covering the most recent six decades (i.e., 1960–2019) with the goal of aligning this study with the temporal coverage of the highest quality reanalysis data sets available. For the remainder of the paper, the results from the two Col cores and the two Summit cores are reported as their respective composite records. The composite annual $\delta^{18}O$, A_n and d-excess records are illustrated on the right side of Figure 1.

2.3. Other Related Data

The annually dated HS ice core records are herein compared to available gridded gauge-based and reanalysis data including the NOAA extended reconstructed SST (ERSST) data set (Huang et al., 2017; https://www.ncei.noaa.gov/products/extended-reconstructed-sst), the Global Precipitation Climatology Center (GPCC) Full Data Product Version 2020 for monthly precipitation totals (Schneider et al., 2022; https://psl.noaa.gov/data/gridded/data.gpcc.html), and the ERA5 monthly reanalysis 500 hPa temperature data set (Hersbach et al., 2020; accessed via the Copernicus Climate Data Store at https://cds.climate.copernicus.eu/#!/home).

For simplicity, only the October through April months (corresponding to the 1960–2019 thermal years) were acquired from each data set as these months correspond to the CB wet season when the mountain range receives 90% of its annual precipitation (Vuille et al., 2008). The October through April average for each grid cell was used to produce annual wet season data sets that can be directly compared to the ice core data (without the need to correct for the thermal year calendar).

Once the gridded data sets were temporally aligned with the ice core data sets, additional corrections were made to improve the subsequent spatiotemporal correlation analyses. Specifically, to reduce the noise of interannual variability all data were smoothed with 3-year running means (3YRMs) and then detrended to remove large wavelength variations that may mask the higher resolution temporal-scale correlations.

3. $\delta^{18}O$-Tropical Climate Relationships

The spatial relationship between Andean ice core $\delta^{18}O$ and SSTs has been shown to be strongest in the tropical Pacific Ocean (Thompson et al., 2013, 2017; Vuille et al., 2003). To demonstrate this using the new HS data, Figure 2 shows the correlation field of the annual isotope records from the new HS Col composite record using the spatiotemporal ERSST data set described in Section 2.3. It is evident from Figure 2 that the most significant correlations occur in the NINO3.4 region of the equatorial Pacific. This is consistent with the findings of Thompson et al. (2017) who looked at a 24-year annually resolved firn core drilled at the HS Col in 2016. Note that Figure 2 only displays the correlation field for the 1960–2019 isotope records from the new Col cores. The $\delta^{18}O$ spatial distribution of correlations for the Summit composite record is virtually identical (Figure S4 in Supporting Information S1). The linear correlation coefficient (r) between the 3YRM, detrended NINO3.4 ERSSTs and HS $\delta^{18}O_{col}$ is r = 0.70 (p-value <0.001), while the NINO3.4 ERSST/$\delta^{18}O_{summit}$ correlation coefficient is r = 0.61 (p-value <0.001). The numerical values of all relevant correlations are provided in Table 1.

Table 1
Two-Tailed Pearson Linear Correlation Coefficients (r) Between Huascarán Ice Core Parameters and Atmospheric and Oceanic Meteorological Data

	NINO3.4 ERSST		Precipitation (over the Amazon)		Precipitation (at Huascarán)		T_{500} (over the Amazon)		T_{500} (at Huascarán)	
	Col	Summit	Col	Summit	Col	Summit	Col	Summit	Col	Summit
$\delta^{18}O$	**0.70**	**0.61**	**−0.68**	**−0.58**	−0.21	−0.14	**0.54**	**0.43**	**0.38**	**0.31**
d-excess	0.08	**−0.33**	0.19	**0.36**	−0.15	−0.01	0.00	**−0.35**	−0.06	**−0.47**
A_n	**−0.38**	−0.10	**0.30**	0.05	0.05	−0.07	**−0.42**	−0.16	**−0.44**	−0.22

Note. T_{500} = temperature at the 500 hPa level. All data were smoothed with 3YRMs and detrended prior to the correlation analysis. **Bold** values indicate 95% significance (p-value ≤0.05).

Only a small area of tropical Atlantic SSTs is significantly correlated to the HS $\delta^{18}O$ record (Figure 2), suggesting that the isotopic signals are primarily influenced by Pacific climate, especially in the NINO3.4 region. However, according to GISS II model experiments by Vuille et al. (2003), the Pacific Ocean supplies only a fraction of the moisture falling as snow at HS, with tropical South America (i.e., the Amazon Basin) and the equatorial Atlantic supplying 58.8% and 27.7%, respectively. Tracing the origins of moisture in ice core records can be inferred from *d*-excess (Masson-Delmotte et al., 2005; Pfahl & Sodemann, 2014), which is an expression of the deviation of the isotopic composition from the global meteoric water line due to kinetic fractionations during water phase changes (Xia & Winnick, 2021). The HS *d*-excess records are compared with the ERSST data set and show positive correlations with the SSTs of the Atlantic but not the Pacific (particularly for the Summit cores; Figure S5 in Supporting Information S1), which suggests the existence of linkages between the Atlantic and precipitation falling on HS. Therefore, the strong NINO3.4 SST/$\delta^{18}O$ relationships are indicative of an ocean-atmosphere teleconnection that serves to modify the water stable isotope ratios enroute to HS from the Atlantic.

It is well known that hydrological conditions over the Amazon Basin are strongly influenced by ENSO activity (Jiménez-Muñoz et al., 2016; Towner et al., 2021), and therefore a direct connection can be made between Pacific climate variability and the HS $\delta^{18}O$ record. It has traditionally been accepted that the dominant control on tropical $\delta^{18}O$ is the intensity of precipitation (i.e., the "amount effect") (Dansgaard, 1964; Rozanski et al., 1993; Schmidt et al., 2007), such that precipitation amount is significantly inversely correlated with $\delta^{18}O$. This can be seen in the HS ice cores, which show a large spatial pattern of negative correlations between $\delta^{18}O$ and precipitation (P) over the Amazon Basin (defined here as the region 5°N–10°S, 75°W–55°W; Figure 3). One of the advantages of the GPCC rainfall data set as opposed to other gauge-based products is that it only incorporates weather station data with continuous records of at least 10 years (Sun et al., 2018). On a global scale, the GPCC data products are integrated with more than 67,000 station records, although their spatial representation is considerably thinner

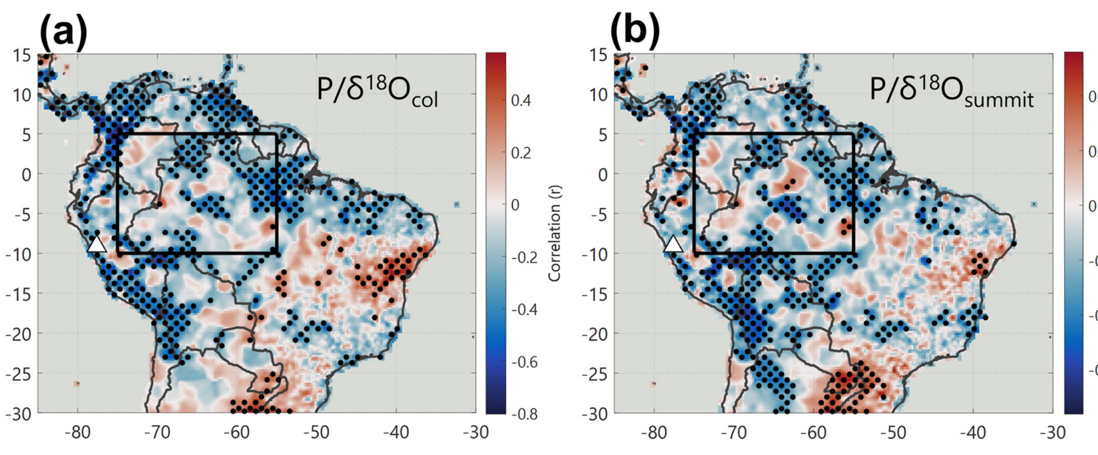

Figure 3. Spatial correlations (0.25° × 0.25°) between wet season precipitation (P) for the period 1960–2019 and (a) the HS $\delta^{18}O_{col}$ composite and (b) the HS $\delta^{18}O_{summit}$ composite. Stipple marks indicate statistical significance at the 95% level (p-value ≤0.05). The black rectangle delimits the approximate bounds of the Amazon Basin (5°N–10°S, 75°W–55°W) as defined for the purposes of this study.

in the low latitudes (Sun et al., 2018). This likely explains the low abundance of statistically significant grid cells over the Amazon region as displayed in Figure 3, as most grid cells in this area contain interpolated data rather than true observations. Nonetheless, GPCC precipitation amounts are consistent (within 5%) with other gauge- and satellite-based data sets across tropical South America (Juárez et al., 2009), meaning that the low volume of stations in the region does not greatly influence the interpretations of our analyses relative to any other data product that may have been chosen.

While the majority of statistically significant correlations of P within the Amazon region are inversely correlated to HS δ^{18}O, some positive correlations are observed. This may be due to uncertainties within the interpolated data points in the GPCC data set or the inhomogeneity of rainfall trends across the basin since the 1980s (Paca et al., 2020). As such, the *average* precipitation trend within the bounds of the Amazon was used to assess the regional relationship between P and HS δ^{18}O. This comparison reveals a correlation coefficient of $r = -0.68$ (p-value <0.001) between P and $\delta^{18}O_{col}$ and $r = -0.58$ (p-value <0.001) between P and $\delta^{18}O_{summit}$. These values are highly consistent with the correlations observed between HS δ^{18}O and ERSSTs in the NINO3.4 region (Table 1). Indeed, the two climatic phenomena cannot be statistically separated, as Amazonian P is strongly related to NINO3.4 ERSSTs ($r = -0.68$, p-value <0.001; Figure S6 in Supporting Information S1). This reflects the ENSO-driven variability of precipitation over the Amazon, such that the warm (cool) phase of ENSO is associated with decreased (enhanced) rainfall over tropical South America (García-García & Ummenhofer, 2015; Ronchail et al., 2002). Thus, the observed P/δ^{18}O correlations would appear to support rainfall amount as a major influence on the stable isotope signals at HS on an annual time scale.

However, because of the equally strong connection with tropical Pacific SSTs, the ice core δ^{18}O record is better defined as a proxy of the ocean-atmosphere system. The causative mechanism for this may be explained by Hurley et al. (2019), who used a proxy system model to interpret the isotopic values of snowfall on the Quelccaya ice cap in southern Peru. Specifically, they found that δ^{18}O is predominantly governed by upstream convection within the western Amazon as a consequence of ENSO variability. For instance, during La Niña the activity of the South American Summer Monsoon (SASM) is enhanced, resulting in lower initial values of δ^{18}O in the vapor that is transported westward to the ice cap (Hurley et al., 2019). The connection between SSTs and Amazonian rainfall is further linked by a strong correlation with trade winds in the western arm of the Pacific Walker circulation belt (Barichivich et al., 2018). According to Towner et al. (2021), during El Niño years anomalously warm Pacific SSTs are related to a weakening of the Walker circulation, thereby driving rainfall-suppressing subsidence over the central and eastern Amazon (Panisset et al., 2018). Conversely, La Niña episodes of ENSO are associated with the convergence of humid air masses over the Amazon (Espinoza et al., 2013) which leads to enhanced precipitation within the basin (Satyamurty et al., 2013). Thus, the HS isotope records may record this mechanistic relationship between SSTs and precipitation over tropical South America.

Interestingly, rainfall amount in the grid cell containing the ice core site does not exhibit any statistically significant relationships with either HS δ^{18}O or the A_n records (Table 1). This observation may be due to the inhomogeneous topography of the Andes, making it difficult to accurately estimate the climatology of a single grid cell (Vuille et al., 2003). Alternatively, these results may be explained by the extreme elevation difference between HS and the observational data incorporated into the GPCC product. Since the ice core sites reside in such a cold, high altitude environment, the isotopic composition of snowfall on HS may be more affected by local atmospheric temperatures than by local precipitation amount (though rainfall amount is the primary driver across the larger region). This would be consistent with the interpretations of δ^{18}O as a temperature recorder in polar ice cores (e.g., Andersen et al., 2004; Johnsen et al., 1995; Lorius et al., 1985; Rasmussen et al., 2013; Watanabe et al., 1999). The results presented here are also consistent with the work of Vargas et al. (2022) who found that the isotopic composition of rainfall in the Ecuadorian Andes is more related to regional precipitation amount than local rainfall, and that decreasing temperatures become the primary driver of isotopic changes during water vapor ascent within the Andes.

To test the relationship between high altitude temperatures and the HS isotopes, the correlation field for 500 hPa temperature (T_{500}) and $\delta^{18}O_{col}$ is shown in Figure 4. The figure clearly reveals that the isotope record from the HS Col is significantly (p-value ≤0.05) correlated with upper atmospheric temperatures over the Amazon Basin, as well as with those in the northern Peruvian Andes (the correlation field for $\delta^{18}O_{summit}$ is largely similar; Figure S7 in Supporting Information S1). Over the Amazon, T_{500} is significantly correlated to the composite δ^{18}O record for the Col (Summit), with an r value of 0.54 (0.43) (the p-value is <0.001 for both). Within the grid cell containing

10.1029/2023JD039006

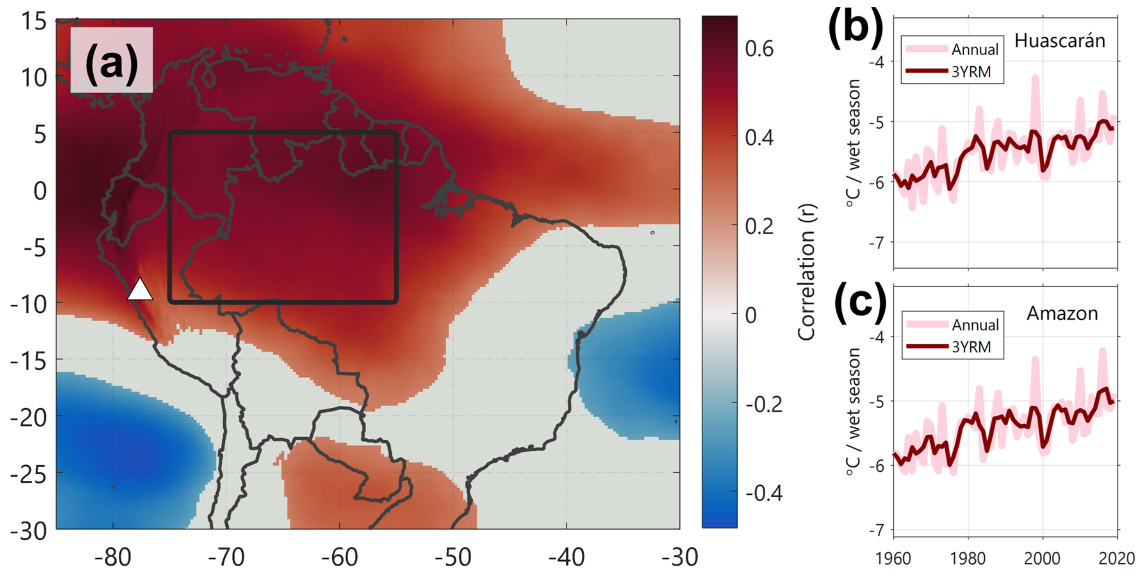

Figure 4. (a) Spatial correlations (0.25° × 0.25°) for T_{500}/$\delta^{18}O_{col}$ during the 1960–2019 wet seasons. Only the grid cells that are statistically significant at the 95% level (p-value ≤0.05) are plotted. (b) Time series of T_{500} in the grid cell containing the ice core site. (c) T_{500} time series for the Amazon Basin (black rectangle on the correlation map, the same area as delimited in Figure 3).

the ice core site, the correlations are weaker but still statistically significant (p-value ≤0.05): $r = 0.38$ (0.31). This is in direct contrast to the P/$\delta^{18}O$ relationships observed at Huascarán itself, which are not statistically significant. The GPCC and ERA5 data sets share the same spatial resolution (0.25° × 0.25°) and thus the size of the grid cell has no effect on these results even though the centers of the grid cells are offset. Moreover, the statistically significant relationship between HS $\delta^{18}O$ and local 500 hPa temperatures and the lack of a statistically significant relationship between HS $\delta^{18}O$ and local precipitation is consistent with the results from Aron et al. (2021) who found that—while upstream precipitation and deep convection within the Amazon are the initial drivers of $\delta^{18}O$ in southern Peru—local rainfall has a negligible influence on the isotopic ratios compared to the decrease in temperature that is associated with increasing elevation in the Andes. Thus, these results lend support to the hypothesis that atmospheric temperatures play a significant role in determining the isotopic composition of snowfall at very high elevations.

4. Multidecadal Variability of the $\delta^{18}O$ Correlations

In the previous section, clear evidence was presented that the HS ice cores are good recorders of tropical Pacific climate variability and by extension they also capture the broad hydrological behavior of the Amazon Basin. However, due to the complexities of ocean-atmosphere interactions and various long-term oceanic oscillations, the relationships described in Section 3 only tell a part of the story. While the HS $\delta^{18}O$ signal is significantly correlated with NINO3.4 ERSSTs, Amazonian rainfall, and 500 hPa temperatures across the full 60-year study period (1960–2019), these relationships are not necessarily constant from a multidecadal perspective.

Figure 5 illustrates the time series of correlations between HS $\delta^{18}O$ and the three previously discussed climate variables that are interrelated through ocean-air processes and the Walker circulation. The correlations are divided into 31 individual 30-year sliding climate intervals (i.e., 1960–1989, 1961–1990, …, 1990–2019). Two interesting patterns emerge from this analysis. First, since 1960, the correlation coefficients between HS $\delta^{18}O$ and each climate parameter exhibit trends of increasing statistical significance. These trends are noteworthy because they suggest that the influence of Pacific climate is not only strengthening on Amazonian climate but also on HS $\delta^{18}O$. A similar pattern displaying this enhanced post-1960 NINO3.4 SST/$\delta^{18}O$ relationship has been reported for the $\delta^{18}O$ chronology of *C. montana* trees in southern Ecuador (Volland et al., 2016). The most significant changes in the correlation trends are centered around the 1980–2009 period. According to the recent IPCC Sixth Assessment Report, it is very likely that the Walker circulation has shifted westward and been strengthening since the 1980s (IPCC, 2021). This is relevant because the Walker circulation acts as a link between equatorial Pacific SSTs and subsidence over the Amazon Basin during El Niño, thereby reducing convective activity (Grimm, 2003). Thus,

10.1029/2023JD039006

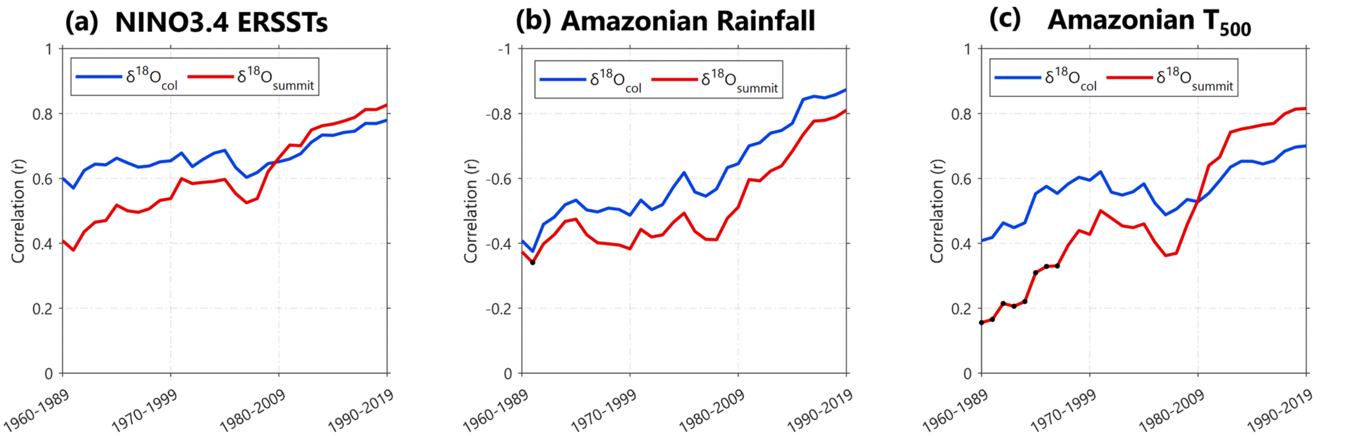

Figure 5. Time series of 30-year multidecadal rolling correlation coefficients between the HS $\delta^{18}O$ composites and (a) NINO3.4 ERSSTs, (b) P over the Amazon Basin, and (c) 500 hPa temperatures over the Amazon Basin. Note that the *y*-axis in (b) is reversed to better illustrate the increasing strength of the correlations toward the present. Black dots denote *r*-values that are not statistically significant at the 95% level (*p*-value ≤0.05).

changes in the Walker circulation may be related directly to this increasing significance of tropical climate/$\delta^{18}O$ correlations.

The second interesting pattern in Figure 5 is that the correlation trends between HS $\delta^{18}O_{summit}$ and the two temperature data sets (i.e., ERSSTs and T_{500}) increase at faster rates than the $\delta^{18}O_{col}$-temperature correlations, especially after the 1980–2009 climate interval. These findings imply that the Summit isotope record has a greater sensitivity to changes in tropical Pacific SSTs and climatological conditions over the Amazon. The rate of increase is highest for $T_{500}/\delta^{18}O_{summit}$ shifting from $r = 0.15$ (not statistically significant) for 1960–1989 to $r = 0.53$ and to $r = 0.82$ for the 1980–2009 and 1990–2019 periods, respectively. The same general pattern is observed when examining T_{500} in the grid cell containing the ice core site (Figure S8 in Supporting Information S1). This rapid rate of change may reflect the observed atmospheric warming trends back to the mid-twentieth century (Gulev et al., 2021). Several studies have found evidence that warming rates in the tropical Andes appear to be enhanced at higher elevations (Aguilar-Lome et al., 2019; Toledo et al., 2022; Urrutia & Vuille, 2009), and the $T_{500}/\delta^{18}O$ relationships may reflect these observations. However, the rate of increasing $T_{500}/\delta^{18}O_{summit}$ correlation coefficients does not necessarily mean that the higher elevation site is warming faster; rather, it simply suggests that warming rates are influencing the isotopes at the Summit more significantly than those at the Col. Thus, these results are not suitable for directly assessing the existence of an elevation-dependent warming mechanism at HS.

5. Contributions to HS $\delta^{18}O$ From ENSO, PDO, and NAO

This study also focused on examining the influence of several large-scale patterns of ocean-atmosphere variability on the HS $\delta^{18}O$ signal. For instance, it is clear from the work of Thompson et al. (2017) and the analysis presented above that the HS isotopes are related to Pacific climate and by extension to the El Niño Southern Oscillation (ENSO). While the El Niño and La Niña episodes of ENSO have an average frequency of around 7 years, the Pacific Decadal Oscillation (PDO) functions similarly to ENSO but extend over longer time intervals. In addition, the North Atlantic Oscillation (NAO) reflects the north-south pressure differences over the Atlantic Ocean (Hurrell et al., 2001). As the tropical North Atlantic is the original moisture source area for a large fraction of the snowfall on HS, phase shifts in the NAO should affect the HS isotope record.

Figure 6 illustrates the annual time series of HS ice core measurements along with the wet season averages for the NAO, PDO, and Southern Oscillation Index (SOI; https://www.ncei.noaa.gov/access/monitoring/products/). The three strongest El Niño events of the last six decades—1982/83, 1997/98, and 2015/16—are marked with vertical black lines. In general, these El Niño events are associated with relatively high (i.e., less-negative) $\delta^{18}O$ and lower *d*-excess values in the HS ice cores. However, A_n is not consistently associated with either positive or negative anomalies during El Niño years. This may be explained by occasional "break downs" in the ENSO-net balance relationship observed in the Cordillera Blanca since the 1970s (Vuille et al., 2008). Alternatively, it may be partially caused by the randomness of post-depositional processes such as the redistribution of snow by wind or melting.

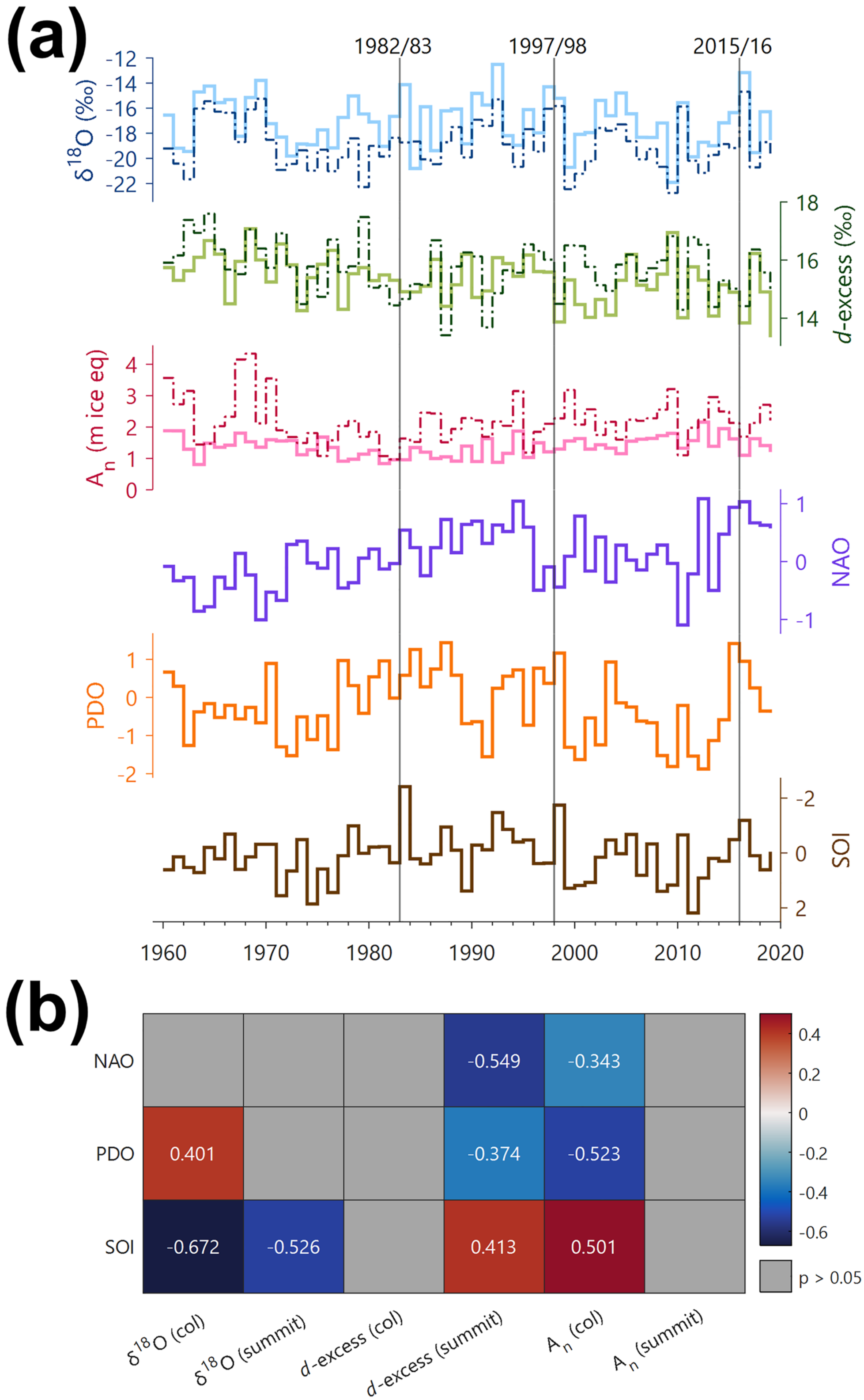

Figure 6. (a) 60-year time series of HS ice core parameters and oceanic climate indices. For the ice core parameters, solid lines correspond to the Col composite record and dashed lines correspond to the Summit composite record. Vertical lines denote very strong El Niño years. The 60-year SOI time series is plotted with an inverted *y*-axis to align with the PDO. (b) Heat map of correlations (3YRM, detrended) that are statistically significant (*p*-value ≤ 0.05).

The statistically significant 60-year correlations (p-value ≤ 0.05) between the HS parameters and the three oceanic indices are visualized at the bottom of Figure 6 (a full visualization of all relationships is given in Figure S9 in Supporting Information S1). The isotopic composition of $\delta^{18}O$ is not strongly influenced by the NAO in either composite core record, which is consistent with the lack of ERSST/$\delta^{18}O$ correlations observed over the Atlantic Ocean in Figure 2. However, the *d*-excess record from the HS Summit is significantly correlated with NAO ($r = 0.55$), although in contrast the Col *d*-excess record is less significantly correlated with NAO and not statistically significant (Figure S9 in Supporting Information S1). Because *d*-excess is not sensitive to changes in elevation (Aron et al., 2021), one potential explanation for this observation is that the lower elevation HS Col receives more recycled continental moisture whereas the 700-m higher Summit site receives a mixture of less recycled continental moisture and more moisture directly of oceanic origin. On the one hand, this possibility should be viewed with caution because moisture recycling is known to increase the value of *d*-excess (Jiménez-Iñiguez et al., 2022) while in general *d*-excess is higher on the Summit than the Col (Figure 1). On the other hand, this inconsistency may reflect higher sublimation rates on the Col than on the Summit as sublimation lowers *d*-excess (Stichler et al., 2001). This has been shown to be especially true in dry, windy environments like Antarctica (Hu et al., 2022). Indeed, windier conditions exist on the HS Col due to the funneling of air between the two mountain peaks. Higher sublimation rates and ice loss due to wind scouring would also explain why lower A_n values are observed on the Col than on the Summit.

Looking at both Pacific indices in Figure 6, the HS $\delta^{18}O$ record is strongly linked to the SOI in both cores ($r = -0.67$, $r = 0.53$ for the Col and Summit, respectively) but only the $\delta^{18}O_{col}$ record displays a statistically significant relationship with the PDO ($r = 0.40$) over the full 60-year period. In any case evidence indicates that the oxygen isotope signal in the HS ice cores is reflective of Pacific climate variability and is influenced by ENSO.

6. Summary and Conclusions

This paper presents the composite $\delta^{18}O$ records of four ice cores collected in 2019 from the world's highest tropical mountain, which provide unique insights into tropical climate variability over the last six decades. This is also the first study to introduce ice core records from the HS Summit and the first to compare the behavior of oxygen stable isotopes in ice cores from different elevations at HS. The composite ice core $\delta^{18}O$ records from both the Col and Summit cores show statistically significant spatiotemporal relationships with Pacific SSTs in the NINO3.4 region, as well as with precipitation and 500 hPa temperatures over tropical South America. Although the tropical North Atlantic is the primary moisture source area for precipitation on HS, we find that Atlantic SSTs do not play a significant role in modulating the $\delta^{18}O$ signals in the HS records. Instead, the dominant drivers of the isotopic values appear to begin with Pacific SSTs and the behavior of ENSO. This is because the strength of the SASM is directly related to ENSO activity and anomalies in the Walker circulation. Subsidence or convergence of moisture over the Amazon (depending on the phase of ENSO) determines the amount upstream convection and thus is the initial control on $\delta^{18}O$. As water vapor is advected to the Andes and uplifted to higher elevations, changes in temperature become the main governing mechanism behind isotopic fractionation. This mechanism is illustrated in Figure S10 in Supporting Information S1.

The analysis shows that the climate/$\delta^{18}O_{col}$ correlations are consistently stronger than the climate/$\delta^{18}O_{summit}$ correlations for the full 1960–2019 period. However, when correlations are examined using a moving window of 30-year climate increments, they reveal that temperature/$\delta^{18}O$ relationships are strengthening at a faster rate at the higher elevation Summit site than at the Col. In particular, the ERSST/$\delta^{18}O$ and T_{500}/$\delta^{18}O$ relationships are strongest in the composite record for the Summit ice cores for the most recent 30-year period (1990–2019). These results suggest that the influence of tropical Pacific climate on the isotopic composition of snowfall on HS is increasing, possibly due to the rapid rates of climate change observed in recent decades. Moreover, the data indicate that $\delta^{18}O$ on the higher elevation Summit is more sensitive than $\delta^{18}O$ on the Col to large-scale changes in tropical Pacific SSTs.

This study contributes to the ongoing discussion of the utility of high altitude, low latitude ice cores and their oxygen stable isotope records. The implications of our findings extend to future studies that seek to reconstruct the complete $\delta^{18}O$ history of the Huascarán ice cores, as well as to modeling approaches that consider the behavior of oxygen isotopes at very high elevations in the tropics.

Data Availability Statement

The ice core data presented in this study can be accessed through the NOAA/WDS-Paleo archive (https://www.ncei.noaa.gov/access/paleo-search/study/38519) and the computer scripts used to calculate accumulation rates and to evaluate spatiotemporal correlations are available at https://zenodo.org/record/8356101 (Weber, 2023).

Acknowledgments
We would like to thank the members of the 2019 Huascarán field expedition team who helped collect the ice cores used in this study, including the many Peruvian porters and mountaineers, without whose support the drilling project would never have been possible. Funding for the 2019 drilling project was provided by the National Science Foundation (NSF) Award #1805819. This is Byrd Polar and Climate Research Center contribution No. C-1627.

References

Aguilar-Lome, J., Espinoza-Villar, R., Espinoza, J.-C., Rojas-Acuña, J., Willems, B. L., & Leyva-Molina, W.-M. (2019). Elevation-dependent warming of land surface temperatures in the Andes assessed using MODIS LST time series (2000–2017). *International Journal of Applied Earth Observation and Geoinformation*, *77*, 119–128. https://doi.org/10.1016/j.jag.2018.12.013

Ampuero, A., Stríkis, N. M., Apaéstegui, J., Vuille, M., Novello, V. F., Espinoza, J. C., et al. (2020). The forest effects on the isotopic composition of rainfall in the Northwestern Amazon Basin. *Journal of Geophysical Research: Atmospheres*, *125*(4), e2019JD031445. https://doi.org/10.1029/2019JD031445

Andersen, K. K., Azuma, N., Barnola, J.-M., Bigler, M., Biscaye, P., Caillon, N., et al. (2004). High-resolution record of Northern Hemisphere climate extending into the last interglacial period. *Nature*, *431*(7005), 147–151. https://doi.org/10.1038/nature02805

Aron, P. G., Poulsen, C. J., Fiorella, R. P., Levin, N. E., Acosta, R. P., Yanites, B. J., & Cassel, E. J. (2021). Variability and controls on δ^{18}O, d-excess, and Δ'^{17}O in southern Peruvian precipitation. *Journal of Geophysical Research: Atmospheres*, *126*(23), e2020JD034009. https://doi.org/10.1029/2020JD034009

Barichivich, J., Gloor, E., Peylin, P., Brienen, R. J. W., Schöngart, J., Espinoza, J. C., & Pattnayak, K. C. (2018). Recent intensification of Amazon flooding extremes driven by strengthened Walker circulation. *Science Advances*, *4*(9), eaat8785. https://doi.org/10.1126/sciadv.aat8785

Cai, W., Wu, L., Lengaigne, M., Li, T., McGregor, S., Kug, J.-S., et al. (2019). Pantropical climate interactions. *Science*, *363*(6430), eaav4236. https://doi.org/10.1126/science.aav4236

Córdova, M., Célleri, R., & van Delden, A. (2022). Dynamics of precipitation anomalies in tropical SouthSouth America. *Atmosphere*, *13*(6), 972. https://doi.org/10.3390/atmos13060972

Dansgaard, W. (1964). Stable isotopes in precipitation. *Tellus*, *16*(4), 436–468. https://doi.org/10.1111/j.2153-3490.1964.tb00181.x

da Rocha Ribeiro, R., Simões, J. C., Ramirez, E., Taupin, J.-D., Assayag, E., & Dani, N. (2018). Accumulation rate in a tropical Andean glacier as a proxy for northern Amazon precipitation. *Theoretical and Applied Climatology*, *132*(1), 569–578. https://doi.org/10.1007/s00704-017-2108-7

Eghdami, M., & Barros, A. P. (2019). Extreme Orographic rainfall in the eastern Andes tied to cold air intrusions. *Frontiers in Environmental Science*, *7*, 101. https://doi.org/10.3389/fenvs.2019.00101

Eltahir, E. A. B., & Bras, R. L. (1994). Precipitation recycling in the Amazon basin. *Quarterly Journal of the Royal Meteorological Society*, *120*(518), 861–880. https://doi.org/10.1002/qj.49712051806

Espinoza, J. C., Ronchail, J., Frappart, F., Lavado, W., Santini, W., & Guyot, J. L. (2013). The major floods in the Amazonas river and tributaries (western Amazon Basin) during the 1970–2012 period: A focus on the 2012 flood. *Journal of Hydrometeorology*, *14*(3), 1000–1008. https://doi.org/10.1175/JHM-D-12-0100.1

Figueroa, S. N., Satyamurty, P., & Dias, P. L. D. S. (1995). Simulations of the summer circulation over the SouthSouth American region with an Eta Coordinate model. *Journal of the Atmospheric Sciences*, *52*(10), 1573–1584. https://doi.org/10.1175/1520-0469(1995)052<1573:SOTSCO>2.0.CO;2

García-García, D., & Ummenhofer, C. C. (2015). Multidecadal variability of the continental precipitation annual amplitude driven by AMO and ENSO. *Geophysical Research Letters*, *42*(2), 526–535. https://doi.org/10.1002/2014GL062451

Grimm, A. M. (2003). The El Niño impact on the summer Monsoon in Brazil: Regional processes versus remote influences. *Journal of Climate*, *16*(2), 263–280. https://doi.org/10.1175/1520-0442(2003)016<0263:TENIOT>2.0.CO;2

Grootes, P. M., Stuiver, M., Thompson, L. G., & Mosley-Thompson, E. (1989). Oxygen isotope changes in tropical ice, Quelccaya, Peru. *Journal of Geophysical Research*, *94*(D1), 1187–1194. https://doi.org/10.1029/JD094iD01p01187

Gulev, S. K., Thorne, P. W., Ahn, J., Dentener, F. J., Domingues, C. M., Gerland, S., et al. (2021). Changing state of the climate system. In V. Masson-Delmotte, P. Zhai, A. Pirani, S. L. Connors, C. Péan, S. Berger, et al. (Eds.), *Climate change 2021: The physical science basis. Contribution of Working Group I to the sixth assessment report of the Intergovernmental Panel on Climate Change* (pp. 287–422). Cambridge University Press.

Henderson, K. A., Thompson, L. G., & Lin, P.-N. (1999). Recording of El Niño in ice core δ18O records from Nevado Huascarán, Peru. *Journal of Geophysical Research*, *104*(D24), 31053–31065. https://doi.org/10.1029/1999JD900966

Hersbach, H., Bell, B., Berrisford, P., Hirahara, S., Horányi, A., Muñoz-Sabater, J., et al. (2020). The ERA5 global reanalysis. *Quarterly Journal of the Royal Meteorological Society*, *146*(730), 1999–2049. https://doi.org/10.1002/qj.3803

Hu, J., Yan, Y., Yeung, L. Y., & Dee, S. G. (2022). Sublimation origin of negative deuterium excess observed in snow and ice samples from McMurdo Dry Valleys and Allan Hills Blue ice areas, East Antarctica. *Journal of Geophysical Research: Atmospheres*, *127*(11), e2021JD035950. https://doi.org/10.1029/2021JD035950

Huang, B., Thorne, P. W., Banzon, V. F., Boyer, T., Chepurin, G., Lawrimore, J. H., et al. (2017). NOAA extended reconstructed sea surface temperature (ERSST), Version 5. https://doi.org/10.7289/V5T72FNM

Hurley, J. V., Vuille, M., & Hardy, D. R. (2019). On the interpretation of the ENSO signal embedded in the stable isotopic composition of Quelccaya Ice Cap, Peru. *Journal of Geophysical Research: Atmospheres*, *124*(1), 131–145. https://doi.org/10.1029/2018JD029064

Hurrell, J. W., Kushnir, Y., & Visbeck, M. (2001). The North Atlantic scillation. *Science*, *291*(5504), 603–605. https://doi.org/10.1126/science.1058761

IPCC. (2021). In P. Valérie Masson-Delmotte, A. Zhai, S. L. Pirani, C. Connors, S. Péan, N. Berger, et al. (Eds.), *Climate change 2021: The physical science basis*. Cambridge University Press.

Jiménez-Iñiguez, A., Ampuero, A., Valencia, B. G., Mayta, V. C., Cruz, F. W., Vuille, M., et al. (2022). Stable isotope variability of precipitation and cave drip-water at Jumandy cave, western Amazon River basin (Ecuador). *Journal of Hydrology*, *610*, 127848. https://doi.org/10.1016/j.jhydrol.2022.127848

Jiménez-Muñoz, J. C., Mattar, C., Barichivich, J., Santamaría-Artigas, A., Takahashi, K., Malhi, Y., et al. (2016). Record-breaking warming and extreme drought in the Amazon rainforest during the course of El Niño 2015–2016. *Scientific Reports*, *6*(1), 33130. https://doi.org/10.1038/srep33130

Johnsen, S. J., Dahl-Jensen, D., Dansgaard, W., & Gundestrup, N. (1995). Greenland palaeotemperatures derived from GRIP bore hole temperature and ice core isotope profiles. *Tellus B: Chemical and Physical Meteorology*, *47*(5), 624–629. https://doi.org/10.3402/tellusb.v47i5.16077
Juárez, R. I. N., Li, W., Fu, R., Fernandes, K., & de Oliveira Cardoso, A. (2009). Comparison of precipitation datasets over the tropical South-South American and African continents. *Journal of Hydrometeorology*, *10*(1), 289–299. https://doi.org/10.1175/2008JHM1023.1
Junquas, C., Takahashi, K., Condom, T., Espinoza, J.-C., Chavez, S., Sicart, J.-E., & Lebel, T. (2018). Understanding the influence of orography on the precipitation diurnal cycle and the associated atmospheric processes in the central Andes. *Climate Dynamics*, *50*(11), 3995–4017. https://doi.org/10.1007/s00382-017-3858-8
Lorius, C., Jouzel, J., Ritz, C., Merlivat, L., Barkov, N. I., Korotkevich, Y. S., & Kotlyakov, V. M. (1985). A 150,000-year climatic record from Antarctic ice. *Nature*, *316*(6029), 591–596. https://doi.org/10.1038/316591a0
Makarieva, A. M., Gorshkov, V. G., & Li, B.-L. (2009). Precipitation on land versus distance from the ocean: Evidence for a forest pump of atmospheric moisture. *Ecological Complexity*, *6*(3), 302–307. https://doi.org/10.1016/j.ecocom.2008.11.004
Marengo, J. A., Souza, C. M., Thonicke, K., Burton, C., Halladay, K., Betts, R. A., et al. (2018). Changes in climate and land use over the Amazon Region: Current and future variability and trends. *Frontiers in Earth Science*, *6*, 228. https://doi.org/10.3389/feart.2018.00228
Masson-Delmotte, V., Landais, A., Stievenard, M., Cattani, O., Falourd, S., Jouzel, J., et al. (2005). Holocene climatic changes in Greenland: Different deuterium excess signals at Greenland Ice Core Project (GRIP) and NorthGRIP. *Journal of Geophysical Research*, *110*(D14), D14102. https://doi.org/10.1029/2004JD005575
Mateo, E. I., Mark, B. G., Hellström, R. Å., Baraer, M., McKenzie, J. M., Condom, T., et al. (2022). High-temporal-resolution hydrometeorological data collected in the tropical Cordillera Blanca, Peru (2004–2020). *Earth System Science Data*, *14*(6), 2865–2882. https://doi.org/10.5194/essd-14-2865-2022
Paca, V. H., da, M., Espinoza-Dávalos, G. E., Moreira, D. M., & Comair, G. (2020). Variability of trends in precipitation across the Amazon river basin determined from the CHIRPS precipitation product and from station records. *Water*, *12*(5), 1244. https://doi.org/10.3390/w12051244
Panisset, J. S., Libonati, R., Gouveia, C. M. P., Machado-Silva, F., França, D. A., França, J. R. A., & Peres, L. F. (2018). Contrasting patterns of the extreme drought episodes of 2005, 2010 and 2015 in the Amazon Basin. *International Journal of Climatology*, *38*(2), 1096–1104. https://doi.org/10.1002/joc.5224
Pfahl, S., & Sodemann, H. (2014). What controls deuterium excess in global precipitation? *Climate of the Past*, *10*(2), 771–781. https://doi.org/10.5194/cp-10-771-2014
Ramirez, E., Hoffmann, G., Taupin, J. D., Francou, B., Ribstein, P., Caillon, N., et al. (2003). A new Andean deep ice core from Nevado Illimani (6350 m), Bolivia. *Earth and Planetary Science Letters*, *212*(3), 337–350. https://doi.org/10.1016/S0012-821X(03)00240-1
Rasmussen, S. O., Abbott, P. M., Blunier, T., Bourne, A. J., Brook, E., Buchardt, S. L., et al. (2013). A first chronology for the North Greenland Eemian Ice Drilling (NEEM) ice core. *Climate of the Past*, *9*(6), 2713–2730. https://doi.org/10.5194/cp-9-2713-2013
Ronchail, J., Cochonneau, G., Molinier, M., Guyot, J.-L., De Miranda Chaves, A. G., Guimarães, V., & de Oliveira, E. (2002). Interannual rainfall variability in the Amazon basin and sea-surface temperatures in the equatorial Pacific and the tropical Atlantic Oceans. *International Journal of Climatology*, *22*(13), 1663–1686. https://doi.org/10.1002/joc.815
Rozanski, K., Araguás-Araguás, L., & Gonfiantini, R. (1993). Isotopic patterns in modern global precipitation. In *Washington DC American Geophysical Union Geophysical Monograph Series*. (Vol. 78, pp. 1–36). https://doi.org/10.1029/GM078p0001
Satyamurty, P., da Costa, C. P. W., Manzi, A. O., & Candido, L. A. (2013). A quick look at the 2012 record flood in the Amazon Basin. *Geophysical Research Letters*, *40*(7), 1396–1401. https://doi.org/10.1002/grl.50245
Schmidt, G. A., LeGrande, A. N., & Hoffmann, G. (2007). Water isotope expressions of intrinsic and forced variability in a coupled ocean-atmosphere model. *Journal of Geophysical Research*, *112*(D10), D10103. https://doi.org/10.1029/2006JD007781
Schneider, U., Hänsel, S., Finger, P., Rustemeier, E., & Ziese, M. (2022). GPCC climatology version 2022 at 0.25°: Monthly land-surface precipitation climatology for every month and the total year from rain-Gauges built on GTS-based and historical data. *GPCC*. https://doi.org/10.5676/DWD_GPCC/FD_M_V2022_025
Stichler, W., Schotterer, U., Fröhlich, K., Ginot, P., Kull, C., Gäggeler, H., & Pouyaud, B. (2001). Influence of sublimation on stable isotope records recovered from high-altitude glaciers in the tropical Andes. *Journal of Geophysical Research*, *106*(D19), 22613–22620. https://doi.org/10.1029/2001JD900179
Sun, Q., Miao, C., Duan, Q., Ashouri, H., Sorooshian, S., & Hsu, K. (2018). A review of global precipitation data sets: Data sources, estimation, and Intercomparisons. *Reviews of Geophysics*, *56*(1), 79–107. https://doi.org/10.1002/2017RG000574
Thompson, L. G., Davis, M. E., Mosley-Thompson, E., Beaudon, E., Porter, S. E., Kutuzov, S., et al. (2017). Impacts of recent warming and the 2015/2016 El Niño on tropical Peruvian ice fields. *Journal of Geophysical Research: Atmospheres*, *122*(23), 12688–12701. https://doi.org/10.1002/2017JD026592
Thompson, L. G., Davis, M. E., Mosley-Thompson, E., Porter, S. E., Corrales, G. V., Shuman, C. A., & Tucker, C. J. (2021). The impacts of warming on rapidly retreating high-altitude, low-latitude glaciers and ice core-derived climate records. *Global and Planetary Change*, *203*, 103538. https://doi.org/10.1016/j.gloplacha.2021.103538
Thompson, L. G., Mosley-Thompson, E., Davis, M. E., Lin, P.-N., Henderson, K. A., Cole-Dai, J., et al. (1995). Late glacial stage and holocene tropical ice core records from Huascaran, Peru. *Science*, *269*(5220), 46–50. https://doi.org/10.1126/science.269.5220.46
Thompson, L. G., Mosley-Thompson, E., Davis, M. E., Zagorodnov, V. S., Howat, I. M., Mikhalenko, V. N., & Lin, P.-N. (2013). Annually resolved ice core records of tropical climate variability over the past 1800 years. *Science*, *340*(6135), 945–950. https://doi.org/10.1126/science.1234210
Toledo, O., Palazzi, E., Cely Toro, I. M., & Mortarini, L. (2022). Comparison of elevation-dependent warming and its drivers in the tropical and subtropical Andes. *Climate Dynamics*, *58*(11), 3057–3074. https://doi.org/10.1007/s00382-021-06081-4
Towner, J., Ficchí, A., Cloke, H. L., Bazo, J., Coughlan de Perez, E., & Stephens, E. M. (2021). Influence of ENSO and tropical Atlantic climate variability on flood characteristics in the Amazon basin. *Hydrology and Earth System Sciences*, *25*(7), 3875–3895. https://doi.org/10.5194/hess-25-3875-2021
Tuinenburg, O. A., Theeuwen, J. J. E., & Staal, A. (2020). High-resolution global atmospheric moisture connections from evaporation to precipitation. *Earth System Science Data*, *12*(4), 3177–3188. https://doi.org/10.5194/essd-12-3177-2020
Urrutia, R., & Vuille, M. (2009). Climate change projections for the tropical Andes using a regional climate model: Temperature and precipitation simulations for the end of the 21st century. *Journal of Geophysical Research*, *114*(D2), D02108. https://doi.org/10.1029/2008JD011021
USGS. (1999). Peruvian Cordilleras. Retrieved https://pubs.usgs.gov/pp/p1386i/peru/occident.html#STEFAN
Valdivielso, S., Vázquez-Suñé, E., & Custodio, E. (2020). Origin and variability of oxygen and hydrogen isotopic composition of precipitation in the central Andes: A review. *Journal of Hydrology*, *587*, 124899. https://doi.org/10.1016/j.jhydrol.2020.124899
Vargas, D., Chimborazo, O., László, E., Temovski, M., & Palcsu, L. (2022). Rainwater isotopic composition in the Ecuadorian Andes and Amazon reflects cross-equatorial flow seasonality. *Water*, *14*(13), 2121. https://doi.org/10.3390/w14132121

Veiga, J. A. P., Rao, V. B., & Franchito, S. H. (2005). Heat and moisture budgets of the Walker circulation and associated rainfall anomalies during El Niño events. *International Journal of Climatology*, *25*(2), 193–213. https://doi.org/10.1002/joc.1115

Volland, F., Pucha, D., & Bräuning, A. (2016). Hydro-climatic variability in southern Ecuador reflected by tree-ring oxygen isotopes. *Erdkunde*, *70*(1), 69–82. https://doi.org/10.3112/erdkunde.2016.01.05

Vuille, M., Bradley, R. S., Healy, R., Werner, M., Hardy, D. R., Thompson, L. G., & Keimig, F. (2003). Modeling δ18O in precipitation over the tropical Americas: 2. Simulation of the stable isotope signal in Andean ice cores. *Journal of Geophysical Research*, *108*(D6), 4175. https://doi.org/10.1029/2001JD002039

Vuille, M., Kaser, G., & Juen, I. (2008). Glacier mass balance variability in the Cordillera Blanca, Peru and its relationship with climate and the large-scale circulation. *Global and Planetary Change*, *62*(1–2), 14–28. https://doi.org/10.1016/j.gloplacha.2007.11.003

Watanabe, O., Kamiyama, K., Motoyama, H., Fujii, Y., Shoji, H., & Satow, K. (1999). The paleoclimate record in the ice core at Dome Fuji station, East Antarctica. *Annals of Glaciology*, *29*, 176–178. https://doi.org/10.3189/172756499781821553

Weber, A. M. (2022). Amazonian influences on the hydrological and mineralogical signals preserved in an ice core from the Cordillera Blanca, Peru (M.S. Thesis). The Ohio State University. Retrieved from http://rave.ohiolink.edu/etdc/view?acc_num=osu1657122127966177

Weber, A. M. (2023). MATLAB scripts for "Drivers of δ^{18}O variability preserved in ice cores from Earth's highest tropical mountain" Version 1.0.0 [Software]. Zenodo. https://doi.org/10.5281/zenodo.8356101

Xia, Z., & Winnick, M. J. (2021). The competing effects of terrestrial evapotranspiration and raindrop re-evaporation on the deuterium excess of continental precipitation. *Earth and Planetary Science Letters*, *572*, 117120. https://doi.org/10.1016/j.epsl.2021.117120

References From the Supporting Information

Bolzan, J. F. (1985). Ice flow at the Dome C ice divide based on a deep temperature profile. *Journal of Geophysical Research*, *90*(D5), 8111–8124. https://doi.org/10.1029/JD090iD05p08111

Cuffey, R. M., & Paterson, W. S. B. (2010). *The physics of glaciers* (4th ed.). Academic Press.

Henderson, K. A. (1996). The El Niño Southern Oscillation and other modes of interannual variability as recorded in ice cores from the Nevado Huascarán col, Peru (M.S. Thesis). The Ohio State University.